# The First Steps of the Visual Cycle in Human Rod and Cone Photoreceptors

Chunhe Chen,[1] Leopold Adler IV,[1] Cole Milliken,[1] Bushra Rahman,[1] Masahiro Kono,[1] Lynn Poole Perry,[1] Federico Gonzalez-Fernandez,[2,3] and Yiannis Koutalos[1]

[1]Department of Ophthalmology, Medical University of South Carolina, Charleston, South Carolina, United States
[2]Departments of Ophthalmology and Pathology, University of Mississippi Medical Center, Jackson, Mississippi, United States
[3]G.V. (Sonny) Montgomery Veterans Affairs Medical Center, Jackson, Mississippi, United States

Correspondence: Yiannis Koutalos, Department of Ophthalmology, Medical University of South Carolina, 167 Ashley Avenue, Charleston, SC 29425, USA; koutalo@musc.edu.

**Received:** February 23, 2024
**Accepted:** June 9, 2024
**Published:** July 3, 2024

Citation: Chen C, Adler L IV, Milliken C, et al. The first steps of the visual cycle in human rod and cone photoreceptors. *Invest Ophthalmol Vis Sci.* 2024;65(8):9. https://doi.org/10.1167/iovs.65.8.9

**Purpose.** Light detection destroys the visual pigment. Its regeneration, necessary for the recovery of light sensitivity, is accomplished through the visual cycle. Release of all-*trans* retinal by the light-activated visual pigment and its reduction to all-*trans* retinol comprise the first steps of the visual cycle. In this study, we determined the kinetics of all-*trans* retinol formation in human rod and cone photoreceptors.

**Methods.** Single living rod and cone photoreceptors were isolated from the retinas of human cadaver eyes (ages 21 to 90 years). Formation of all-*trans* retinol was measured by imaging its outer segment fluorescence (excitation, 360 nm; emission, >420 nm). The extent of conversion of released all-*trans* retinal to all-*trans* retinol was determined by measuring the fluorescence excited by 340 and 380 nm. Measurements were repeated with photoreceptors isolated from *Macaca fascicularis* retinas. Experiments were carried out at 37°C.

**Results.** We found that ~80% to 90% of all-*trans* retinal released by the light-activated pigment is converted to all-*trans* retinol, with a rate constant of 0.24 to 0.55 $min^{-1}$ in human rods and ~1.8 $min^{-1}$ in human cones. In *M. fascicularis* rods and cones, the rate constants were 0.38 ± 0.08 $min^{-1}$ and 4.0 ± 1.1 $min^{-1}$, respectively. These kinetics are several times faster than those measured in other vertebrates. Interphotoreceptor retinoid-binding protein facilitated the removal of all-*trans* retinol from human rods.

**Conclusions.** The first steps of the visual cycle in human photoreceptors are several times faster than in other vertebrates and in line with the rapid recovery of light sensitivity exhibited by the human visual system.

Keywords: rod photoreceptors, cone photoreceptors, retinol, retinal, visual cycle

The human retina contains two kinds of photoreceptor cells: rods and cones.[1] The one type of rod and the three types of cones are each sensitive to a different range of light wavelengths. Rods have high sensitivity to light and are responsible for vision in dim light, whereas cones have low light sensitivity and are responsible for vision at the high light intensities of daytime and for color discrimination. Conversion of light to an electrical signal takes place in the photoreceptor outer segments, which are packed with visual pigment molecules, the primary light-detectors.[2] Visual pigments are composed of a light-sensitive chromophore, 11-*cis* retinal, attached to a protein, opsin. Each of the four photoreceptor types contains a different type of visual pigment, all of which, however, contain the same 11-*cis* retinal chromophore. The different properties of the different types of visual pigments are due to different types of opsins. Light detection proceeds in the same way in both rods and cones: Incoming light absorbed by the visual pigment isomerizes the chromophore from 11-*cis* to all-*trans*, bringing about a conformational change in the visual pigment that initiates a cascade of reactions culminating in a change in membrane potential; the electrical signal is then transmitted to the brain. At the same time, the photoisomerization of the chromophore to all-*trans* destroys the visual pigment and necessitates its regeneration. Visual pigment regeneration is essential for the recovery of visual sensitivity after light exposure,[3] a process critical for carrying out daily tasks and one that deteriorates with age.[4] Visual pigment regeneration is much faster in humans and non-human primates compared to several other mammalian species (for a summary, see Ref. 3).

The reactions regenerating the pigment are known as the visual cycle[5] and begin with the release of all-*trans* retinal from the light-activated visual pigment, leaving behind opsin, which is then available to combine with fresh 11-*cis* retinal and regenerate the visual pigment. Upon its release, all-*trans* retinal is reduced to all-*trans* retinol in a reaction catalyzed by retinol dehydrogenase 8 (RDH8)[6–9] and using nicotinamide adenine dinucleotide phosphate

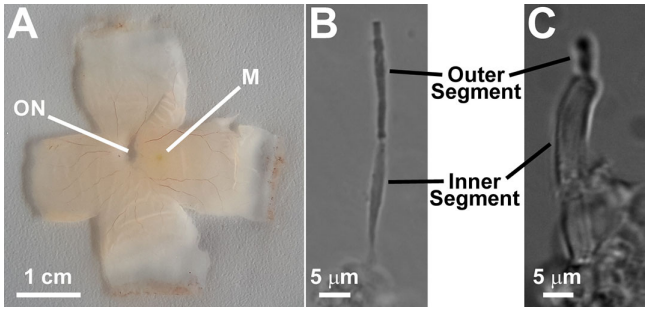


**Figure 1.** Images of isolated human retina (**A**) and isolated human rod (**B**) and cone (**C**) photoreceptors. ON, optic nerve spot; M, macula. Phototransduction, the conversion of light to an electrical signal, takes place in the photoreceptor outer segments, which contain the light-detecting visual pigments. The inner segments contain the metabolic machinery that supports outer segment function, including the supply of NADPH.

(NADPH),[10] and initiating the series of reactions that recycle the chromophore into fresh 11-*cis* retinal. All-*trans* retinol is removed from photoreceptor outer segments and transported to the adjacent retinal pigment epithelial (RPE) or Müller cells,[5] where it is recycled to reform the 11-*cis* isomers, 11-*cis* retinal in the RPE cells[11] or 11-*cis* retinol in the Müller cells.[12,13] Both rods and cones can utilize 11-*cis* retinal supplied to them by RPE cells[5]; cones can also utilize 11-*cis* retinol supplied by the Müller cells,[14,15] because they are able to oxidize it to 11-*cis* retinal.[16] Defects in the processing of the visual pigment chromophore are linked to diseases of the retina,[17,18] with the slower regeneration of the visual pigment in particular being one of the early symptoms of age-related macular degeneration.[19]

The first steps of the visual cycle in photoreceptor outer segments—namely, the release of all-*trans* retinal from photoactivated pigment that makes opsin available for regeneration and the formation of all-*trans* retinol that begins the recycling of the chromophore—are expected to be sufficiently rapid to support the overall kinetics of visual pigment regeneration. In mouse rods, all-*trans* retinol forms with a rate constant of 0.06 $min^{-1}$ after light exposure,[20] sufficiently fast to accommodate the kinetics of rhodopsin regeneration in mouse retinas but too slow compared to that in human retinas (see Discussion). We therefore hypothesized that formation of all-*trans* retinol proceeds much faster in human rod photoreceptors compared to mouse.

The levels of all-*trans* retinol and all-*trans* retinal can be measured with high resolution in real time in single photoreceptor cells by imaging their fluorescence.[21] Here, we report on the characterization of the kinetics of all-*trans* retinol formation in single rod and cone photoreceptor cells isolated from human donor eyes (Fig. 1) with fluorescence imaging. We have corroborated our findings with photoreceptor cells isolated from the eyes of a non-human primate, *Macaca fascicularis*. We find that, in human rod and cone photoreceptors, the all-*trans* retinal released from the photoactivated pigment is quantitatively converted to all-*trans* retinol. This conversion to all-*trans* retinol proceeds several times faster in human compared to mouse rods, paralleling the faster recovery of sensitivity after light exposure in humans. The results indicate that the enzymatic machinery of human photoreceptors effectively and rapidly removes the all-*trans* retinal generated during light detection, making it available for speedy recycling.

## Materials and Methods

### Human Donor Eyes

Donor eyes were procured through the National Disease Research Interchange. Eyes were from donors without diagnosed eye disease or diabetes mellitus. Retinas from human donor eyes were subject to a long and variable period of ischemia, which might affect the responses of the cells. We addressed this by adhering to the following protocol: Eyes were enucleated within 10 hours postmortem and placed in moist chambers labeled to specify whether the globes were left or right. They were then shipped to the laboratory on ice in a light-tight container and dissected within 48 hours after donor death. Upon inspection the retinas did not show any signs of pathology. Eyes from 12 donors, male and female, ages 21 to 90 years, were used in this study. The study used available eyes, so any potential effects of donor sex could not be properly studied.

### *Macaca fascicularis* Eyes

*M. fascicularis* eyes were obtained from Alpha Genesis (Yemassee, SC, USA), located within an hour's drive from the laboratory. Tissue was procured when animals were sacrificed for another purpose; the animals were free of eye disease or any conditions related to visual dysfunction. Eyes were removed immediately following euthanasia and placed in moist chambers labeled to specify whether the globes were left or right. They were brought to the laboratory on ice in a light-tight container and were dissected within 3 to 4 hours after death. From experiments with retinas from three animals, we determined that following this protocol dissected retinas contain 75% ± 7% unbleached rhodopsin. Animals were male and female and ages ranged from 2 to 19 years.

### Measurement of the Level of Unbleached Rhodopsin in *M. fascicularis* Retinas

All procedures were carried out under dim red light. Following isolation of the retina and separation of the macula for experiments with cones, a large piece (about 1/4) of the rod-rich perimacular region was homogenized in PBS (10-mmol/L sodium phosphate and 150-mmol/L NaCl, pH 7.0) and split into two aliquots of 300 µL each. To one of the aliquots, 5 nmol of 11-*cis* retinal (1 µL from a stock solution of 5 mM in ethanol) was added, and to the other 1 µL of ethanol was added. Each aliquot was then mixed and incubated for 20 minutes at room temperature. After the incubation, the retinal membranes of each aliquot were solubilized in 0.66% dodecylmaltoside in PBS, hydroxylamine was added to a final concentration of 15 mM, and spectra were recorded between 250 and 700 nm with a Cary 300 spectrophotometer (Varian, Palo Alto, CA, USA). The amount of rhodopsin in each aliquot was measured from the difference in the absorbance at 500 nm before and after bleaching the samples with >530 nm light. The ratio of the amount of rhodopsin in the unregenerated sample over the amount in the 11-*cis* retinal–regenerated sample was used as the estimate for the level of unbleached rhodopsin present in the retina.

Investigative Ophthalmology & Visual Science

### Isolation of Single Rod and Cone Photoreceptor Cells

Retinas were excised under either dim red or infrared light in mammalian physiological solution (130-mmol/L NaCl, 5-mmol/L KCl, 0.5-mmol/L $MgCl_2$, 2-mmol/L $CaCl_2$, 25-mmol/L HEPES hemisodium salt, and 5-mmol/L glucose, pH = 7.40) and kept in a light-tight container at 4°C until they were used for the isolation of cells.[20] The macular region (Fig. 1) was identified by noting the position of the optic nerve, knowing whether the eye was left or right, and keeping track of tissue orientation during dissection (the macula is on the temporal side of the optic nerve between the retinal arcades). Rod photoreceptors were isolated from the rod-rich area surrounding the macula, and cone photoreceptors from the cone-rich center of the macula (Ref. 1, p. 43, based on Ref. 22). Single photoreceptor cells were obtained by chopping a piece of retina with a razor blade in a dish coated with Sylgard elastomer (Dow Corning Corporation, Midland, MI, USA) and placed in 100-µL chambers that fit on the microscope stage.[20] To keep the cells in place during experimental manipulations, the bottoms of the chambers were coated with 0.01% polyornithine solution (Sigma-Aldrich, St. Louis, MO, USA). For the experiments described here, the photoreceptors used were isolated within the first 2 days after dissection of the retina. Within this time period, the cells maintained their ability to generate the amount of NADPH required for the quantitative reduction of all-*trans* retinal to all-*trans* retinol.

### Fluorescence Imaging

Fluorescence imaging experiments were carried out as described previously[20] on the stage of an inverted Zeiss Axiovert 100 microscope (Carl Zeiss Microscopy, White Plains, NY, USA) with a 40× oil immersion objective lens (numerical aperture = 1.3). A xenon continuous arc light source provided the light for excitation, and an Orca-285 charge-coupled device (CCD) camera (Hamamatsu Photonics, Bridgewater, NJ, USA) was used to acquire images. For measuring all-*trans* retinol, fluorescence was excited with a broadband (40-nm bandwidth) 360-nm filter, and the emission was collected through a long-pass 420-nm filter (emission, >420 nm). The particular broadband excitation of 360 nm was selected because it allows for comparison with previously published data from a wide range of species. For measuring the Fex-340/Fex-380 ratio of the fluorescence intensities excited by 340-nm and 380-nm light, fluorescence was excited with narrow bandpass (10-nm bandwidth) filters centered at 340 nm and 380 nm, and emission was collected for >420 nm. Most experiments were carried out with photoreceptors, with the outer segment attached to an intact inner segment, which ensured access to NADPH; these cells are also referred to as metabolically intact.[23] Some experiments (Supplementary Fig. S1) used broken-off rod outer segments (bROSs), outer segments completely separated from inner segments and therefore without access to NADPH; these rod outer segments are also referred to as metabolically compromised.[23] For human bROSs, the Fex-340/Fex-380 ratio at 10 minutes after bleaching was 0.47 ± 0.03 ($n$ = 9), consistent with that for all-*trans* retinal, indicating that there was no significant reduction of all-*trans* retinal to all-*trans* retinol. We were able to collect reliable data for the Fex-340/Fex-380 ratio, but we did not attempt to characterize the kinetics of the fluorescence change after bleaching in bROSs. Rods isolated from human donor eyes have small amounts of rhodopsin present, and, because of the lower quantum yield, the intensity of fluorescence due to retinal is much lower than that of the same concentration of retinol. Thus, metabolically compromised human rods generate a very small fluorescence signal after bleaching, making it difficult to reliably detect and analyze.

For an experiment, fluorescence images were initially recorded for the dark-adapted cell, then the cell was bleached and fluorescence images were recorded at different times. The bleaching light came from a 150-W halogen lamp illuminator (Edmund Optics, Barrington, NJ, USA), using >530 nm light for 1 minute for rods and white light for 15 seconds for cones. Image acquisition and analysis were carried out using Slidebook (Intelligent Imaging Innovations, Denver, CO, USA). Fluorescence intensity was measured over defined regions of interest in the outer segments and background; after correcting for background, the initial value before bleaching was subtracted from all subsequent values to obtain the fluorescence due to retinoids. All experiments were carried out at 37°C.

### Kinetics of All-*trans* Retinol Formation

We approximated the formation and elimination of all-*trans* retinol following light activation of the visual pigment as two separate first-order processes with rate constants $f_1$ and $f_2$[20,24,25]:

$$\text{Visual pigment} \xrightarrow{light} \text{Photoactivated pigment} \xrightarrow{f_1} \text{All-trans retinol} \xrightarrow{f_2} \text{Bulk solution} \quad (1)$$

In our experiments, formation of the light-activated pigment by light was much faster than the formation and elimination of all-*trans* retinol; in addition, >90% of the outer segment visual pigment is photoisomerized and activated by the bleaching light.[20,25] In that case, the concentration of all-*trans* retinol [*ROL*] at time $t$ after visual pigment bleaching is given by

$$[ROL] = \frac{[P]_T \cdot f_1}{f_1 - f_2} \cdot \left(e^{-f_2 \cdot t} - e^{-f_1 \cdot t}\right)$$

where $[P]_T$ is the total concentration of the visual pigment in the photoreceptor outer segment, ~3 mM. The outer segment fluorescence ($F$) due to all-*trans* retinol is given by

$$F = \frac{A \cdot f_1}{f_1 - f_2} \cdot \left(e^{-f_2 \cdot t} - e^{-f_1 \cdot t}\right) \quad (2)$$

where the parameter $A$ is the outer segment fluorescence intensity that would correspond to the total amount of retinyl chromophore released by the photoactivated pigment. Values of the parameters $A$, $f_1$, and $f_2$ were determined by least-squares fits of the time course of the average fluorescence intensity values using Origin software (OriginLab Corporation, Northampton, MA, USA). Errors for parameters were obtained from the curve fits. Another approach for determining the values of the parameters is to fit the time course of the fluorescence intensity values for each cell, obtain the kinetic parameters for each cell, and then average the individual cell parameters. The two approaches yield similar results.

### Removal of All-*trans* Retinol by Interphotoreceptor Retinoid-Binding Protein

The human rod photoreceptors used for these determinations had not been regenerated with exogenously added 11-*cis* retinal. Interphotoreceptor retinoid-binding protein (IRBP) was added to the rods 10 minutes after the bleaching of rhodopsin. The outer segment all-*trans* retinol fluorescence was normalized to the value at 11 minutes, and the rate constant $k$ for all-*trans* retinol removal was determined by fitting the normalized fluorescence values obtained after 11 minutes with single-exponential functions, $e^{-k\cdot(t-11)}$, of unitary amplitude at $t = 11$ minutes.[25,26] We chose the particular experimental design not only to allow for direct comparisons with the results from mouse cells[26] but also to ensure that the cells generated a strong fluorescence signal to allow for reliable analysis. For example, if we were to add IRBP from the beginning of the experiment, we would expect very low levels of outer segment retinoid fluorescence (Ref. 26, fig. 8), which would have been compounded by the small amounts of rhodopsin present in isolated human rods.

### Regeneration With 11-*cis* Retinal

For some experiments, the visual pigment of isolated human photoreceptors was regenerated with 11-*cis* retinal by incubating the cells (after they had been placed in the experimental chambers) with 2.5- or 5-µM 11-*cis* retinal for 10 minutes using IRBP in physiological solution as the carrier; the IRBP concentration was twice the concentration of 11-*cis* retinal. At the end of the incubation, IRBP and 11-*cis* retinal were removed by washing the cells three times with physiological solution. These incubations were carried out at room temperature. Interestingly, regeneration with a higher concentration of 11-*cis* retinal did not result in a higher level of rhodopsin in all cases.

### Materials

IRBP was purified from bovine interphotoreceptor matrix by a combination of concanavalin-A, affinity, anion exchange, and size-exclusion chromatography and was used as described previously.[26] The 11-*cis* retinal was obtained through a National Eye Institute program that makes it available for vision research; its concentration was determined from its absorption spectrum measured with the Cary 300 spectrophotometer and using an extinction coefficient of 24,935 $M^{-1}$ $cm^{-1}$ at 380 nm in ethanol.[27] All other reagents were obtained from Sigma-Aldrich.

### Statistical Analysis

Error bars represent SEM.

## Results

### Formation of All-*trans* Retinol in Single Isolated Human Rod Photoreceptors

Exposure of isolated human rod photoreceptors to light (>530-nm light for 1 minute) results in a transient increase in the outer segment fluorescence (emission, >420 nm) excited by 360-nm light (Fig. 2A). Figure 2B shows the time-course of changes in the outer segment fluorescence from seven

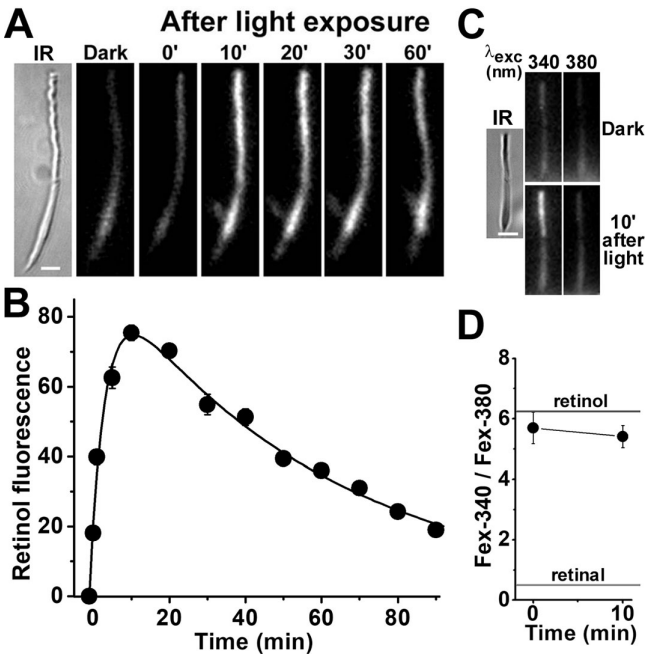


**Figure 2.** Kinetics of all-*trans* retinol formation in isolated human rod photoreceptors. (**A**) Increase in rod outer segment fluorescence after rhodopsin bleaching. IR, infrared image of a rod photoreceptor isolated from a human donor retina (age 80 years); fluorescence (excitation, 360 nm; emission, >420 nm) images of the cell were acquired before (dark) and at different times after bleaching. All fluorescence images are shown at the same intensity scaling. *Scale bar*: 5 µm. (**B**) Kinetics of the fluorescence appearing after bleaching of rhodopsin in the outer segments of human rod photoreceptors ($n = 7$; donor age 80 years). Bleaching was carried out between $t = -1$ and 0 minute. *Error bars* represent standard errors. All experiments were conducted at 37°C. The *solid line* is a least-squares fit according to Equation 2, giving a rate constant for the rise in fluorescence of 0.25 ± 0.02 $min^{-1}$. (**C**) Excitation of outer segment fluorescence with 340-nm and 380-nm light (emission, >420 nm). IR, infrared image of a human rod photoreceptor (donor age 76 years); fluorescence images of the cell were acquired before (dark) and at 10 minutes after bleaching of rhodopsin. Images are shown at the same intensity scaling to facilitate comparisons. *Scale bar*: 5 µm. (**D**) Ratio of the intensities of the fluorescence excited by 340-nm (Fex-340) and 380-nm (Fex-380) light in human rod outer segments ($n = 8$; donor age 76 years) after rhodopsin bleaching. Bleaching was carried out between $t = -1$ and 0 minute. *Error bars* represent standard errors. The fluorescence intensity ratios determined for all-*trans* retinal and all-*trans* retinol (Supplementary Fig. S1) are also shown. All experiments were conducted at 37°C.

rod cells isolated from the same donor. The fluorescence rose and reached a peak ~10 minutes after bleaching of the visual pigment and then declined slowly. A least-squares fit with Equation 2 (see Methods) gave $f_1 = 0.25 \pm 0.02$ $min^{-1}$ for the rate constant for the rise in fluorescence, and $f_2 = 0.017 \pm 0.001$ $min^{-1}$ for the rate constant for the decline. Experiments with isolated rods from two other donors gave values of 0.50 ± 0.05 $min^{-1}$ and 0.53 ± 0.10 $min^{-1}$ for the rising phase rate constant $f_1$, whereas the values for the falling phase rate constant $f_2$ were 0.013 ± 0.001 $min^{-1}$ and 0.022 ± 0.003 $min^{-1}$ (Table, unregenerated). To ensure that the increase in rod outer segment fluorescence originated mostly from all-*trans* retinol, we measured the ratio of the fluorescence >420 nm that is excited by 340 nm (Fex-340) and 380 nm (Fex-380). Because all-*trans* retinol and all-*trans* retinal fluoresce with very different excitation

**Table.** Values of the Parameters Describing The Kinetics of All-*trans* Retinol Formation in Human Rod Photoreceptors Isolated From Different Donors

| Donor Age (y) | 11-*cis* Retinal | Cells, *n* | $f_1$ (min$^{-1}$) | $f_2$ (min$^{-1}$) | *A* |
|---|---|---|---|---|---|
| Ungenerated | | | | | |
| 90 | — | 6 | 0.50 ± 0.05 | 0.013 ± 0.001 | 47 ± 1 |
| 80 | — | 4 | 0.53 ± 0.10 | 0.022 ± 0.003 | 19 ± 1 |
| 80 | — | 7 | 0.25 ± 0.02 | 0.017 ± 0.001 | 91 ± 3 |
| Regenerated | | | | | |
| 21 | 5 µM | 9 | 0.26 ± 0.04 | 0.008 ± 0.001 | 99 ± 5 |
| 78 | 5 µM | 4 | 0.44 ± 0.05 | 0.012 ± 0.001 | 65 ± 2 |
| | 2.5 µM | 4 | 0.55 ± 0.09 | 0.013 ± 0.001 | 28 ± 1 |
| 88 | 5 µM | 5 | 0.24 ± 0.05 | 0.013 ± 0.003 | 50 ± 4 |
| | 2.5 µM | 5 | 0.33 ± 0.09 | 0.002 ± 0.003 | 77 ± 7 |

For three of the donors, cells were not regenerated with 11-*cis* retinal prior to the measurement of all-*trans* retinol formation (unregenerated). For another three donors, cells were regenerated by incubating for 10 minutes with 2.5- or 5-µM 11-*cis* retinal (regenerated). All experiments were conducted at 37°C. The parameters are as follows: $f_1$, rate constant for retinol formation; $f_2$, rate constant for retinol removal; and *A*, fluorescence corresponding to the amount of rhodopsin present before bleaching. Parameters were determined from least-square fits of Equation 2 to the experimental data points (as in Figs. 2B, 3B).

wavelength maxima, the Fex-340/Fex-380 fluorescence ratio provides a measure of the fraction of the all-*trans* retinal released by the light-activated visual pigment converted to all-*trans* retinol.[6,23] The experiment in Figure 2C shows that the outer segment fluorescence generated after exposure of an isolated human rod photoreceptor to light (>530 nm for 1 minute) was much more effectively excited by the 340-nm light, consistent with an all-*trans* retinol origin (Supplementary Fig. S1). Figure 2D shows the values of the Fex-340/Fex-380 ratios for the outer segment fluorescence generated immediately after and 10 minutes after visual pigment bleaching ($n = 8$ rods, isolated from the same donor). These ratio values of ~5 to 6 are similar to those measured in the outer segments of mouse rod photoreceptors and indicate that ~80% to 90% of the released all-*trans* retinal was converted to all-*trans* retinol.[23] The quantitative conversion of all-*trans* retinal to all-*trans* retinol also indicates that the isolated human rod photoreceptors used in these experiments had the metabolic capacity to generate the large amounts of NADPH necessary for the conversion.

For the majority of donor eyes, isolated rod photoreceptors did not generate a significant increase in outer segment fluorescence after the bleaching of rhodopsin, presumably due to excessive exposure to light prior to arrival in the laboratory. In those cases, we recorded a robust outer segment fluorescence signal after regeneration of the isolated rod cells with 11-*cis* retinal. Figure 3A shows an experiment with an isolated human rod photoreceptor after it was regenerated with 5-µM 11-*cis* retinal. Following bleaching of the cell with >530-nm light for 1 minute, there was a transient increase in outer segment fluorescence (excitation, 360-nm; emission, >420-nm). Figure 3B shows the average of the outer segment fluorescence change from four rod cells from the same donor retina after their regeneration with 5-µM 11-*cis* retinal. The fit with Equation 2 gave values of $f_1 = 0.44 \pm 0.05$ min$^{-1}$ and $f_2 = 0.012 \pm 0.001$ min$^{-1}$ for the rate constants for the rise and decline of outer segment fluorescence, respectively. Experiments with four isolated rods from the same donor but regenerated with 2.5-µM 11-*cis* retinal, gave values of $f_1 = 0.55 \pm 0.09$ min$^{-1}$ and $f_2 = 0.013 \pm 0.001$ min$^{-1}$ for the two rate constants. Additional experiments with rods isolated from two more donors and regenerated with either 2.5- or 5-µM 11-*cis* retinal gave broadly similar values for the rising and falling phase rate constants $f_1$ and $f_2$ (Table, regenerated). Most of the outer segment fluorescence that appeared in the 11-*cis* retinal–regenerated rod cells after bleaching was due to all-*trans* retinol, as shown from measurements of the Fex-340/Fex-380 ratio (Figs. 3C, 3D), indicating that ~80% to 90% of the retinal was converted to retinol.

We corroborated these findings with rod photoreceptors isolated from *M. fascicularis* retinas (Fig. 4), which contained ~75% unbleached rhodopsin. Analysis of the all-*trans* retinol formation kinetics gave values of $f_1 = 0.38 \pm 0.08$ min$^{-1}$ and $f_2 = 0.011 \pm 0.002$ min$^{-1}$ for the rate constants for the rise and decline of outer segment fluorescence, respectively (Fig. 4B). The values of the Fex-340/Fex-380 fluorescence ratio were also ~5 to 6 (Fig. 4D), corresponding to ~80% to 90% conversion of released all-*trans* retinal to all-*trans* retinol.

## Removal of All-*trans* Retinol by IRBP

In the absence of extracellular carriers, the all-*trans* retinol that forms in human rod outer segments following exposure to light leaves the cell slowly, resulting in a decline in outer segment fluorescence (Figs. 2A, 2B). This process can be accelerated by the specialized carrier protein IRBP. Figure 5A shows rapid decline of outer segment fluorescence (excitation, 360 nm; emission, >420 nm) after the addition of 3-µM IRBP in the extracellular medium. Following the addition of 3-µM IRBP, outer segment fluorescence declines with a rate constant $k = 0.08 \pm 0.01$ min$^{-1}$ (Fig. 5B). The addition of 13-µM IRBP results in even faster decline of fluorescence, with a rate constant $k = 0.22 \pm 0.04$ min$^{-1}$ (Fig. 5B).

## Formation of All-*trans* Retinol in Single Isolated Human Cone Photoreceptors

Obtaining viable single cones from human donor eyes was significantly more challenging than obtaining rods. We were able to record a transient increase in outer segment fluorescence after light exposure after regeneration of isolated cone cells with 11-*cis* retinal. After incubation with 11-*cis* retinal (2.5-µM for 10 minutes), exposure of a cone cell to white light for 15 seconds resulted in a rapid transient increase in outer segment fluorescence (excitation, 360 nm; emission, >420 nm) (Fig. 6A). The average of the change in outer segment fluorescence from three cone cells from

Investigative Ophthalmology & Visual Science

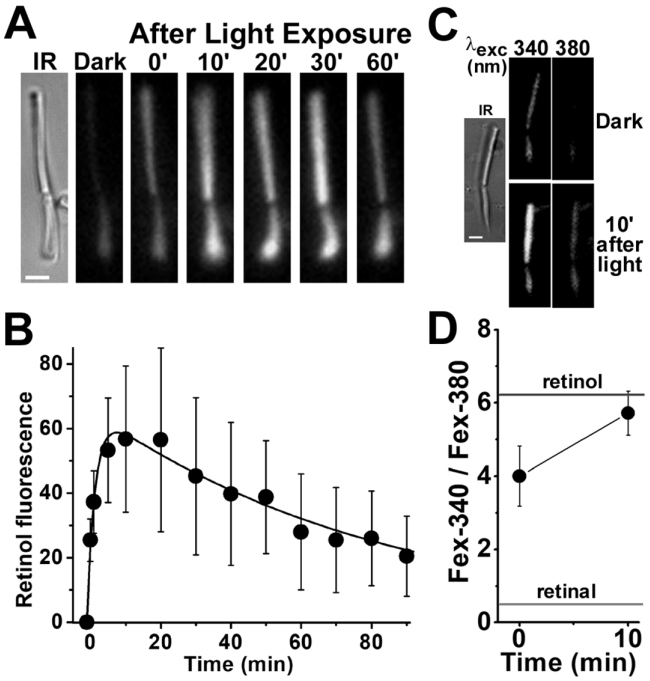


**Figure 3.** Kinetics of all-*trans* retinol formation in isolated human rod photoreceptors that had been regenerated with 11-*cis* retinal. (**A**) Increase in outer segment fluorescence after rhodopsin bleaching in a human rod photoreceptor (donor age 78 years) regenerated with 11-*cis* retinal (5 µM for 10 minutes). IR, infrared image of the cell; fluorescence (excitation, 360 nm; emission, >420 nm) images of the cell were acquired before (dark) and at different times after bleaching. All fluorescence images are shown at the same intensity scaling. *Scale bar*: 5 µm. (**B**) Kinetics of the fluorescence appearing after bleaching of rhodopsin in the outer segments of human rod photoreceptors regenerated with 11-*cis* retinal (5 µM for 10 minutes; $n = 4$; donor age 78 years). Bleaching was carried out between $t = -1$ and 0 minute. *Error bars* represent standard errors. All experiments were conducted at 37°C. The *solid line* is a least-squares fit according to Equation 2, giving a rate constant for the rise in fluorescence of $0.44 \pm 0.05$ min$^{-1}$. (**C**) Excitation of outer segment fluorescence with 340-nm and 380-nm light (emission, >420 nm). IR, infrared image of a human rod photoreceptor (donor age 89 years) regenerated with 11-*cis* retinal (2.5 µM for 10 minutes); fluorescence images of the cell were acquired before (dark) and at 10 minutes after bleaching of rhodopsin. Images are shown at the same intensity scaling to facilitate comparisons. *Scale bar*: 5 µm. (**D**) Ratio of the intensities of the fluorescence excited by 340-nm (Fex-340) and 380-nm (Fex-380) light in human rod outer segments ($n = 5$; donor age 89 years) after rhodopsin bleaching; the rod cells had been regenerated with 11-*cis* retinal (2.5 µM for 10 minutes). Bleaching was carried out between $t = -1$ and 0 minute. *Error bars* represent standard errors. The fluorescence intensity ratios determined for all-*trans* retinal and all-*trans* retinol (Supplementary Fig. S1) are also shown. All experiments were conducted at 37°C.

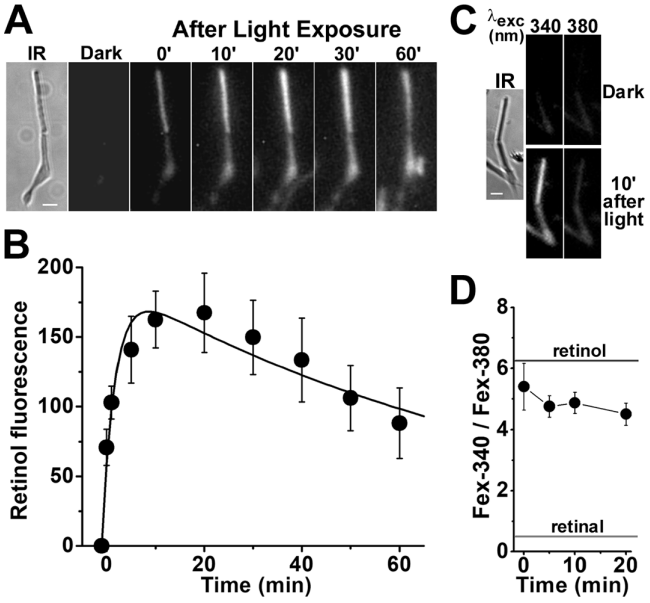


**Figure 4.** Kinetics of all-*trans* retinol formation in *M. fascicularis* rod photoreceptors isolated from dark-adapted eyes. (**A**) Increase in rod outer segment fluorescence after rhodopsin bleaching. IR, infrared image of an isolated *M. fascicularis* rod photoreceptor; fluorescence (excitation, 360 nm; emission, >420 nm) images of the cell were acquired before (dark), and at different times after bleaching; bleaching was carried out between $t = -1$ and 0 minute. All fluorescence images are shown at the same intensity scaling. *Scale bar*: 5 µm. (**B**) Kinetics of the fluorescence appearing after bleaching of rhodopsin in the outer segments of isolated *M. fascicularis* rod photoreceptors ($n = 7$). Bleaching was carried out between $t = -1$ and 0 minute. *Error bars* represent standard errors. All experiments were conducted at 37°C. The *solid line* is a least-squares fit according to Equation 2, giving a rate constant for the rise in fluorescence of $f_1 = 0.38 \pm 0.08$ min$^{-1}$ and a rate constant for the decline of $f_2 = 0.011 \pm 0.002$ min$^{-1}$. (**C**) Excitation of outer segment fluorescence with 340-nm and 380-nm light (emission >420 nm). IR, infrared image of an isolated *M. fascicularis* rod photoreceptor; fluorescence images of the cell were acquired before (dark) and at 10 minutes after the bleaching of rhodopsin. Images are shown at the same intensity scaling to facilitate comparisons. *Scale* bar: 5 µm. (**D**) Ratio of the intensities of the fluorescence excited by 340-nm (Fex-340) and 380-nm (Fex-380) light in *M. fascicularis* rod outer segments ($n = 7$) after rhodopsin bleaching. Bleaching was carried out between $t = -1$ and 0 minute. *Error bars* represent standard errors. The fluorescence intensity ratios determined for all-*trans* retinal and all-*trans* retinol (Supplementary Fig. S1) are also shown. All experiments were conducted at 37°C.

the same donor retina after their regeneration with 2.5-µM 11-*cis* retinal is shown in Figure 6B. Following the bleaching of visual pigment, cone outer segment fluorescence rises rapidly, reaches a peak within ~1 minute, and then declines slowly. A least-squares fit with Equation 2 gave $f_1 = 1.8 \pm 0.1$ min$^{-1}$ for the rate constant for the rise in fluorescence and $f_2 = 0.05 \pm 0.01$ min$^{-1}$ for the rate constant for the decline. As in rod cells, most of the outer segment fluorescence that appeared in the 11-*cis* retinal–regenerated cone cells after bleaching was due to all-*trans* retinol, as shown from measurements of the Fex-340/Fex-380 ratio (Figs. 6C, 6D), again corresponding to ~80% to 90% of retinal converted to retinol. We had more success at isolating viable single cones from *M. fascicularis* retinas; furthermore, those cells did not require regeneration with 11-*cis* retinal to produce an outer segment fluorescence signal (Fig. 7). The rate constants for the rise and decline of outer segment fluorescence in *M. fascicularis* cones were $f_1 = 4.0 \pm 1.1$ min$^{-1}$ and $f_2 = 0.04 \pm 0.01$ min$^{-1}$, respectively, and 80% to 90% of the released retinal was converted to retinol.

## Discussion

The conversion of all-*trans* retinal to all-*trans* retinol requires NADPH[10] and hence depends on the ability of the metabolic machinery of the photoreceptor cells to generate the NADPH necessary to reduce the large amount of all-*trans* retinal released from photoactivated visual pigment after a

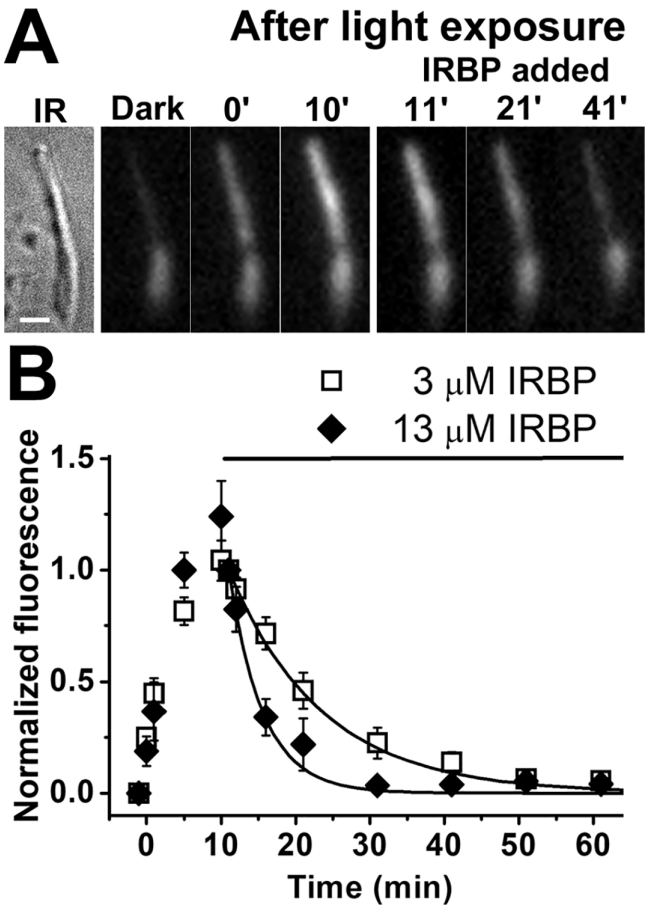


**Figure 5.** Removal of all-*trans* retinol from human rod photoreceptor outer segments by IRBP. (**A**) Removal of all-*trans* retinol formed after rhodopsin bleaching by 3-μM IRBP. IR, infrared image of a single human rod photoreceptor (donor age 69 years). *Scale bar*: 5 μm. Bleaching was carried out between $t = -1$ and 0 minute, and IRBP was added 10 minutes after bleaching. Fluorescence images of the cell (excitation, 360 nm; emission, >420 nm) are shown at the same intensity scaling. (**B**) Removal of all-*trans* retinol by 3-μM IRBP (□; $n = 8$; donor age 69 years) and 13-μM IRBP (♦; $n = 5$; donor age 82 years) added at $t = 10$ minutes after the bleaching of rhodopsin. Retinol outer segment fluorescence intensities have been normalized over the value at $t = 11$ minutes, 1 minutes after the addition of IRBP. *Error bars* denote standard errors. The lines are simple exponentials, $e^{-k\cdot(t-11)}$, decaying to 0 with unitary amplitude at $t = 11$ minutes, with rate constants $k$ determined by the data points. The rate constants were 0.08 ± 0.01 $min^{-1}$ for 3-μM IRBP and 0.22 ± 0.04 $min^{-1}$ for 13-μM IRBP. All experiments were conducted at 37°C.

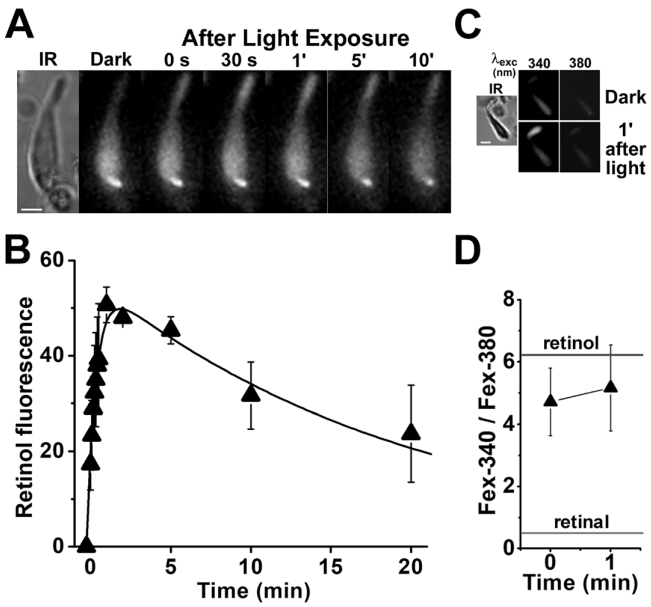


**Figure 6.** Kinetics of all-*trans* retinol formation in isolated human cone photoreceptors that had been regenerated with 11-*cis* retinal. (**A**) Increase in outer segment fluorescence after visual pigment bleaching in a human cone photoreceptor (donor age 85 years) regenerated with 11-*cis* retinal (2.5 μM for 10 minutes). IR, infrared image of the cell; fluorescence (excitation, 360 nm; emission, >420 nm) images of the cell were acquired before (dark) and at different times after bleaching. All fluorescence images are shown at the same intensity scaling. *Scale bar*: 5 μm. (**B**) Kinetics of the fluorescence appearing after the bleaching of visual pigment in the outer segments of human cone photoreceptors regenerated with 11-*cis* retinal (2.5 μM for 10 minutes; $n = 3$; donor age 85 years). Bleaching was carried out between $t = -0.25$ and 0 minute. *Error bars* represent standard errors. All experiments were conducted at 37°C. The *solid line* is a least-squares fit according to Equation 2, giving a rate constant for the rise in fluorescence of 1.8 ± 0.1 $min^{-1}$. (**C**) Excitation of outer segment fluorescence with 340-nm and 380-nm light (emission, >420 nm). IR, infrared image of a human cone photoreceptor (donor age 89 years) regenerated with 11-*cis* retinal (2.5 μM for 10 minutes); fluorescence images of the cell were acquired before (dark) and at 1 minute after bleaching of visual pigment. Images are shown at the same intensity scaling to facilitate comparisons. (**D**) Ratio of the intensities of the fluorescence excited by 340-nm (Fex-340) and 380-nm (Fex-380) light in human cone outer segments ($n = 7$; donor age 89 years) after visual pigment bleaching; the cone cells had been regenerated with 11-*cis* retinal (2.5 μM for 10 minutes). Bleaching was carried out between $t = -0.25$ and 0 minute. *Error bars* represent standard errors. The fluorescence intensity ratios determined for all-*trans* retinal and all-*trans* retinol (Supplementary Fig. S1) are also shown. All experiments were conducted at 37°C.

full bleach. Because of the prolonged period of ischemia endured by the human donor eyes used in our studies, the ability of photoreceptors isolated from them to generate the required NADPH is of concern. The adequacy of NADPH generation can be assessed from the extent of all-*trans* retinal conversion to all-*trans* retinol.[6,23] There is a high (~80% to 90%) conversion of the released all-*trans* retinal to all-*trans* retinol for both rod and cone photoreceptors from both human and *M. fascicularis* cells, as illustrated by the Fex-340/Fex-380 fluorescence ratio values of ~5 after visual pigment bleaching (Figs. 2D, 3D, 4D, 6D, 7D). These values of the ratio are also similar to those measured in rod photoreceptors isolated from dark-adapted mice,[23] whose retinas were dissected immediately after death and thereby subject to virtually no ischemia. Therefore, there is no discernible impairment in the ability of the isolated human photoreceptor cells used in this study to generate the necessary levels of NADPH. The extent of conversion of all-*trans* retinal to all-*trans* retinol is a measure of the level of NADPH, with the conversion of 80% to 90% corresponding to a 0.1 to 0.2 reduced fraction of NADP,[23] which is in good agreement with histochemical measurements.[28] It should be noted that the quantitative (80%–90%) and fast conversion of the all-*trans* retinal released from photoactivated visual pigment to all-*trans* retinol indicates that the enzymatic mechanisms present in human rod and cone photoreceptors efficiently remove all-*trans* retinal, a reactive and cytotoxic aldehyde,[29] and thus guard against it.

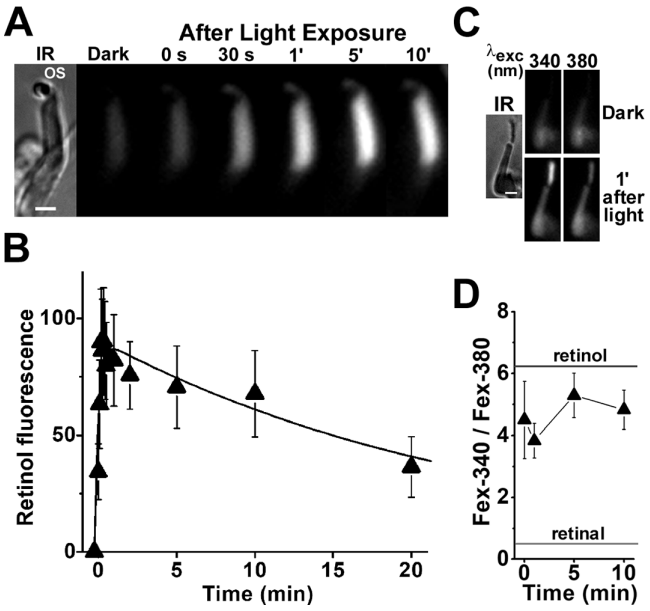


**Figure 7.** Kinetics of all-*trans* retinol formation in *M. fascicularis* cone photoreceptors isolated from dark-adapted eyes. (**A**) Increase in cone outer segment fluorescence after visual pigment bleaching. IR, infrared image of an isolated *M. fascicularis* cone photoreceptor; OS denotes the outer segment of the cell. Fluorescence (excitation, 360 nm; emission, >420 nm) images of the cell were acquired before (dark) and at different times after bleaching, which was carried out between $t = -0.25$ and 0 minute. All fluorescence images are shown at the same intensity scaling. *Scale bar*: 5 µm. (**B**) Kinetics of the fluorescence appearing after bleaching of visual pigment in the outer segments of isolated *M. fascicularis* cone photoreceptors ($n = 5$). Bleaching was carried out between $t = -0.25$ and 0 minute. *Error bars* represent standard errors. All experiments were conducted at 37°C. The *solid line* is a least-squares fit according to Equation 2, giving a rate constant for the rise in fluorescence of $f_1 = 4.0 \pm 1.1$ min$^{-1}$ and a rate constant for the decline of $f_2 = 0.04 \pm 0.01$ min$^{-1}$. (**C**) Excitation of outer segment fluorescence with 340-nm and 380-nm light (emission, >420 nm). IR, infrared image of an isolated *M. fascicularis* cone photoreceptor; fluorescence images of the cell were acquired before (dark) and at 1 minute after the bleaching of visual pigment. Images are shown at the same intensity scaling to facilitate comparisons. *Scale bar*: 5 µm. (**D**) Ratio of the intensities of the fluorescence excited by 340-nm (Fex-340) and 380-nm (Fex-380) light in *M. fascicularis* cone outer segments ($n = 10$) after visual pigment bleaching. Bleaching was carried out between $t = -0.25$ and 0 minute. *Error bars* represent standard errors. The fluorescence intensity ratios determined for all-*trans* retinal and all-*trans* retinol (Supplementary Fig. S1) are also shown. All experiments were conducted at 37°C.

The ability of the isolated human photoreceptor cells to generate the large amounts of NADPH needed for the reduction of all-*trans* retinal to all-*trans* retinol suggests a functional metabolic machinery, which should also generate adenosine triphosphate (ATP). Thus, it is unlikely that ABCA4 activity, which is ATP dependent,[30,31] is compromised. A decline in ABCA4 activity could potentially result in a transient buildup in all-*trans* retinal, which however was not detected. The relatively stable values of the Fex-340/Fex-380 ratio at the early time points after light exposure suggest that there is no transient buildup of all-*trans* retinal. Rather, as all-*trans* retinal is released from the light-activated pigment, it is reduced to all-*trans* retinol, rapidly reaching thermodynamic equilibrium—as is also the case in mouse rods.[23] It is possible that some of the released all-*trans* retinal forms Schiff base with phosphatidylethanolamine, but biochemical experiments with rod outer segment membranes detected no Schiff base formation by the all-*trans* retinal released from light-activated rhodopsin in the presence of NADPH.[32]

In several rod cells, there was an increase in inner segment fluorescence after the bleaching of rhodopsin (for example, Figs. 2A, 3A, 4A), which likely represents all-*trans* retinol and retinal leakage from the outer to the inner segment, as previously seen in mouse rods.[6] Such leakage underscores the important protective role for inner segment retinol dehydrogenases, such as RDH12, which would clear all-*trans* retinal flowing in from the outer segment. RDH12 mutations have been associated with Leber congenital amaurosis, a degeneration of the retina.[33,34] Unfortunately, we were not able to determine the Fex-340/Fex-380 ratios for this inner segment fluorescence signal, as its intensity was not sufficient.

In human rod photoreceptors that contained sufficient amounts of rhodopsin to allow measurements without regeneration with 11-*cis* retinal, all-*trans* retinol formed with a rate constant $f_1$ of 0.25 to 0.53 min$^{-1}$ (Fig. 2B, Table); similar rate constants, 0.24 to 0.55 min$^{-1}$, were obtained from rod cells regenerated with 11-*cis* retinal (Fig. 3B, Table). Because of the variable amounts of rhodopsin present in different cell preparations, we considered the possibility that the faster kinetics of all-*trans* retinol formation were associated with cells that contained smaller amounts of rhodopsin, thus requiring less NADPH. The level of rhodopsin present can be estimated from the value of the parameter $A$ in Equation 2 (listed in the Table), or, alternatively, from the peak value of the outer segment fluorescence after bleaching (shown in Supplementary Fig. S2). Overall, there did not appear to be a major impact of the level of rhodopsin on the rate constant $f_1$ for all-*trans* retinol formation, including for cells from the same donor (Table). In addition, the kinetics of all-*trans* retinol formation in *M. fascicularis* rods, isolated from retinas with ~75% of rhodopsin unbleached, were very similar (Fig. 4B), with a rate constant $f_1$ of 0.38 min$^{-1}$, well within the range measured from human rods. This good agreement also suggests that any effects of the long period of retinal ischemia on human rod photoreceptor function had a minimal impact on the kinetics of all-*trans* retinol formation. Thus, the measured kinetics of all-*trans* retinol formation in human rods are unlikely to be significantly affected by either rhodopsin levels or the prolonged period of retinal ischemia prior to cell isolation. It was not possible to rigorously examine a possible dependence of all-*trans* retinol formation on donor age. Almost all of the data are from photoreceptor cells obtained from donors older than 78 years. Nevertheless, measurements from a single younger donor (21 years) are consistent with the rest.

In the human eye, after the bleaching of rhodopsin during the process of light detection, the recovery of light sensitivity is determined by the regeneration of rhodopsin from opsin and 11-*cis* retinal.[3] Because all-*trans* retinol is formed from the all-*trans* retinal released by the light-activated rhodopsin, its appearance reflects the availability of opsin for regeneration with fresh 11-*cis* retinal. Therefore, following the bleaching of rhodopsin, the rate constant for opsin availability will be at least $f_1$, corresponding to a half-time of less than $\ln 2/f_1 \approx 1.3$ to 2.8 minutes. This is sufficiently fast to allow the regeneration of rhodopsin and the recovery of light sensitivity to proceed with a half-time of ~6 minutes (Ref. 3, figs. 9 and 10); it also reflects the rapid completion

Investigative Ophthalmology & Visual Science

of the first of the series of reactions that recycle the retinyl chromophore and reform 11-*cis* retinal.

The rate constant $f_1$ of 0.25 to 0.53 $min^{-1}$ of all-*trans* retinol formation in isolated human rods is several times faster than that measured in isolated wild-type mouse rods, 0.06 $min^{-1}$.[20] The difference in all-*trans* retinol formation kinetics does not appear to be due to differences in NADPH availability, given the similar extent, 80% to 90%, of all-*trans* retinal to all-*trans* retinol conversion in both human and mouse rods. Thus, it is likely that the difference in kinetics reflects a faster release of all-*trans* retinal from light-activated human rhodopsin compared to mouse. The slower kinetics of all-*trans* retinol formation in mouse rods are in line with the slower regeneration of rhodopsin in mouse eyes, which proceeds with a half-time of ~20 minutes (Ref. 3, fig. 22).

The presence of IRBP in the extracellular space greatly facilitated the removal of all-*trans* retinol from human rod outer segments in a concentration-dependent manner (Fig. 5), as has been shown previously with photoreceptor cells from other species.[24–26,35] Although the experiments utilized IRBP purified from bovine retinas, we do not expect the heterologous origin to have a major effect on the results, as the bovine protein is 84% identical to the human.[36] For the experiments, one of the IRBP concentrations, 13 µM, was chosen because it is reported to be the concentration in human subretinal space.[37] The other concentration, 3 µM, was chosen to provide an additional comparison with results from experiments with mouse rod cells and is the concentration reported in rat subretinal space.[37] The rate constants for the removal of all-*trans* retinol from human rods by 3-µM and 13-µM IRBP (0.08 $min^{-1}$ and 0.22 $min^{-1}$, respectively) are slightly higher than the ones that would be expected for the removal from mouse rods (Ref. 26, fig. 3). This points to possible differences in the removal process in the two species. One possible difference may be in the putative receptor that mediates the removal by IRBP,[25] and yet another may be in the known structural differences between human and mouse rod outer segments, such as the number and depth of incisures.[38,39] It is important to note that the rate constant of 0.22 $min^{-1}$ for the removal of all-*trans* retinol by 13-µM IRBP, the reported physiological concentration, is in good agreement with the time constant of 50 to 300 seconds for the removal estimated from in vivo measurements in *Macaca mulatta* retinas.[40]

The human retina contains three types of cone photoreceptor cells, which are sensitive to long (L), middle (M), and short (S) wavelengths (also known as red-, green- and blue-sensitive cones, respectively).[1] S-cones comprise about 10% of the total cone population and are absent from the center of the fovea; there are about two to four times as many L-cones as M-cones.[1] So, although we were not able to discriminate among the different types of cone cells, we expect L and M to be the types with which our experiments were carried out. Because L and M visual pigments are highly homologous, we also expect the kinetics of all-*trans* retinal release from light-activated visual pigment to be similar, and therefore the kinetics of all-*trans* retinol formation, as well. We made no attempt to classify the cone cells according to their morphology, which varies considerably across the retina (Ref. 41, p. 206, based on Ref. 42). In human cone cells, all-*trans* retinol formed with a rate constant $f_1$ of ~1.8 $min^{-1}$ (Fig. 6B), smaller than the rate constant of 4.0 $min^{-1}$ measured in *M. fascicularis* cones (Fig. 7B) but within the range of variability in rate constants that would be expected from the results with rods. These $f_1$ values are comparable to those measured for the red- and blue-sensitive cones from the larval tiger salamander retina (2.6 and 1.4 $min^{-1}$, respectively) (Ref. 24, table I). These kinetics of all-*trans* retinol formation indicate that, following light detection, cone opsin becomes available for regeneration with a half-time of less than $\ln 2/f_1 \approx 0.4$ minutes, which is sufficiently fast to allow the regeneration of cone visual pigment and the recovery of light sensitivity to proceed with a half-time of ~1 minute (Ref. 3, fig. 11).

In summary, we have determined the kinetics of the first steps of the reactions responsible for the regeneration of the visual pigments of the human rod and cone photoreceptors after exposure to light. As we hypothesized, these kinetics are much faster than those in mouse rod photoreceptors and can support the overall kinetics of visual pigment regeneration. The swift completion of these initial steps is essential for diurnal vision. First, it allows for the rapid recovery of sensitivity to light supporting the continuous vision necessary for daily activities. Second, it accomplishes the rapid removal of the large amounts of all-*trans* retinal, a reactive and cytotoxic aldehyde, released by the light-activated visual pigments. The importance of the speed of these reactions is highlighted by the severe diseases of vision associated with their impairment, as well as by the difficulties experienced when the recovery of light sensitivity is slower than normal.

## Acknowledgments

The 11-*cis* retinal was obtained through a National Eye Institute program.

Supported by a grant from the National Institutes of Health Grant (EY014850 to YK) and an Activation Award from the Veterans Affairs Office of Research Development (to FG-F). YK is the Barbara and Stanley Andrie Endowed Chair for Bioengineering and Vision Research in the Vision SmartState Center of Economic Excellence.

Disclosure: **C. Chen**, None; **L. Adler IV**, None; **C. Milliken**, None; **B. Rahman**, None; **M. Kono**, None; **L.P. Perry**, None; **F. Gonzalez-Fernandez**, None; **Y. Koutalos**, None

## References

1. Rodieck RW. *The First Steps in Seeing*. Sunderland, MA: Sinauer Associates; 1998.
2. Ebrey T, Koutalos Y. Vertebrate photoreceptors. *Prog Retin Eye Res*. 2001;20:49–94.
3. Lamb TD, Pugh EN, Jr. Dark adaptation and the retinoid cycle of vision. *Prog Retin Eye Res*. 2004;23:307–380.
4. Jackson GR, Owsley C, McGwin G, Jr. Aging and dark adaptation. *Vision Res*. 1999;39:3975–3982.
5. Tang PH, Kono M, Koutalos Y, Ablonczy Z, Crouch RK. New insights into retinoid metabolism and cycling within the retina. *Prog Retin Eye Res*. 2013;32:48–63.
6. Chen C, Thompson DA, Koutalos Y. Reduction of all-*trans*-retinal in vertebrate rod photoreceptors requires the combined action of RDH8 and RDH12. *J Biol Chem*. 2012;287:24662–24670.
7. Kolesnikov AV, Maeda A, Tang PH, Imanishi Y, Palczewski K, Kefalov VJ. Retinol dehydrogenase 8 and ATP-binding cassette transporter 4 modulate dark adaptation of M-cones in mammalian retina. *J Physiol*. 2015;593:4923–4941.
8. Maeda A, Maeda T, Imanishi Y, et al. Role of photoreceptor-specific retinol dehydrogenase in the retinoid cycle *in vivo*. *J Biol Chem*. 2005;280:18822–18832.

9. Rattner A, Smallwood PM, Nathans J. Identification and characterization of all-*trans*-retinol dehydrogenase from photoreceptor outer segments, the visual cycle enzyme that reduces all-*trans*-retinal to all-*trans*-retinol. *J Biol Chem*. 2000;275:11034–11043.
10. Futterman S, Hendrickson A, Bishop PE, Rollins MH, Vacano E. Metabolism of glucose and reduction of retinaldehyde in retinal photoreceptors. *J Neurochem*. 1970;17:149–156.
11. Saari JC. Biochemistry of visual pigment regeneration: the Friedenwald lecture. *Invest Ophthalmol Vis Sci*. 2000;41:337–348.
12. Das SR, Bhardwaj N, Kjeldbye H, Gouras P. Muller cells of chicken retina synthesize 11-cis-retinol. *Biochem J*. 1992;285:907–913.
13. Wang JS, Kefalov VJ. The cone-specific visual cycle. *Prog Retin Eye Res*. 2011;30:115–128.
14. Wang JS, Estevez ME, Cornwall MC, Kefalov VJ. Intra-retinal visual cycle required for rapid and complete cone dark adaptation. *Nat Neurosci*. 2009;12:295–302.
15. Wang JS, Kefalov VJ. An alternative pathway mediates the mouse and human cone visual cycle. *Curr Biol*. 2009;19:1665–1669.
16. Miyazono S, Shimauchi-Matsukawa Y, Tachibanaki S, Kawamura S. Highly efficient retinal metabolism in cones. *Proc Natl Acad Sci USA*. 2008;105:16051–16056.
17. Thompson DA, Gal A. Vitamin A metabolism in the retinal pigment epithelium: genes, mutations, and diseases. *Prog Retin Eye Res*. 2003;22:683–703.
18. Travis GH, Golczak M, Moise AR, Palczewski K. Diseases caused by defects in the visual cycle: retinoids as potential therapeutic agents. *Annu Rev Pharmacol Toxicol*. 2007;47:469–512.
19. Owsley C, Jackson GR, White M, Feist R, Edwards D. Delays in rod-mediated dark adaptation in early age-related maculopathy. *Ophthalmology*. 2001;108:1196–1202.
20. Chen C, Blakeley LR, Koutalos Y. Formation of all-*trans* retinol after visual pigment bleaching in mouse photoreceptors. *Invest Ophthalmol Vis Sci*. 2009;50:3589–3595.
21. Adler L, IV, Boyer NP, Chen C, Koutalos Y. Kinetics of rhodopsin's chromophore monitored in a single photoreceptor. *Methods Mol Biol*. 2015;1271:327–343.
22. Oesterberg G. Topography of the layer of rods and cones in the human retina. *Acta Ophthal Kbh Suppl*. 1935;6:1–102.
23. Adler L, IV, Chen C, Koutalos Y. Mitochondria contribute to NADPH generation in mouse rod photoreceptors. *J Biol Chem*. 2014;289:1519–1528.
24. Ala-Laurila P, Kolesnikov AV, Crouch RK, et al. Visual cycle: dependence of retinol production and removal on photoproduct decay and cell morphology. *J Gen Physiol*. 2006;128:153–169.
25. Wu Q, Blakeley LR, Cornwall MC, Crouch RK, Wiggert BN, Koutalos Y. Interphotoreceptor retinoid-binding protein is the physiologically relevant carrier that removes retinol from rod photoreceptor outer segments. *Biochemistry*. 2007;46:8669–8679.
26. Chen C, Adler L, IV, Goletz P, Gonzalez-Fernandez F, Thompson DA, Koutalos Y. Interphotoreceptor retinoid-binding protein removes all-*trans*-retinol and retinal from rod outer segments, preventing lipofuscin precursor formation. *J Biol Chem*. 2017;292:19356–19365.
27. Gundersen TE, Blomhoff R. Qualitative and quantitative liquid chromatographic determination of natural retinoids in biological samples. *J Chromatogr A*. 2001;935:13–43.
28. Matschinsky FM. Quantitative histochemistry of nicotinamide adenine nucleotides in retina of monkey and rabbit. *J Neurochem*. 1968;15:643–657.
29. Chen Y, Okano K, Maeda T, et al. Mechanism of all-*trans*-retinal toxicity with implications for Stargardt disease and age-related macular degeneration. *J Biol Chem*. 2012;287:5059–5069.
30. Quazi F, Lenevich S, Molday RS. ABCA4 is an *N*-retinylidene-phosphatidylethanolamine and phosphatidylethanolamine importer. *Nat Commun*. 2012;3:925.
31. Weng J, Mata NL, Azarian SM, Tzekov RT, Birch DG, Travis GH. Insights into the function of Rim protein in photoreceptors and etiology of Stargardt's disease from the phenotype in *abcr* knockout mice. *Cell*. 1999;98:13–23.
32. Hong JD, Salom D, Kochman MA, Kubas A, Kiser PD, Palczewski K. Chromophore hydrolysis and release from photoactivated rhodopsin in native membranes. *Proc Natl Acad Sci USA*. 2022;119:e2213911119.
33. Janecke AR, Thompson DA, Utermann G, et al. Mutations in *RDH12* encoding a photoreceptor cell retinol dehydrogenase cause childhood-onset severe retinal dystrophy. *Nat Genet*. 2004;36:850–854.
34. Perrault I, Hanein S, Gerber S, et al. Retinal dehydrogenase 12 (*RDH12*) mutations in Leber congenital amaurosis. *Am J Hum Genet*. 2004;75:639–646.
35. Tsina E, Chen C, Koutalos Y, et al. Physiological and microfluorometric studies of reduction and clearance of retinal in bleached rod photoreceptors. *J Gen Physiol*. 2004;124:429–443.
36. Si JS, Borst DE, Redmond TM, Nickerson JM. Cloning of cDNAs encoding human interphotoreceptor retinoid-binding protein (IRBP) and comparison with bovine IRBP sequences. *Gene*. 1989;80:99–108.
37. Adler AJ, Edwards RB. Human interphotoreceptor matrix contains serum albumin and retinol-binding protein. *Exp Eye Res*. 2000;70:227–234.
38. Cohen AI. The ultrastructure of the rods of the mouse retina. *Am J Anat*. 1960;107:23–48.
39. Cohen AI. New details of the ultrastructure of the outer segments and ciliary connectives of the rods of human and macaque retinas. *Anat Rec*. 1965;152:63–79.
40. Sharma R, Schwarz C, Hunter JJ, Palczewska G, Palczewski K, Williams DR. Formation and clearance of all-*trans*-retinol in rods investigated in the living primate eye with two-photon ophthalmoscopy. *Invest Ophthalmol Vis Sci*. 2017;58:604–613.
41. Wyszecki G, Stiles WS. *Color Science: Concepts and Methods, Quantitative Data and Formulas*. New York: John Wiley & Sons; 1967.
42. Polyak SL. *The Retina*. Chicago: University of Chicago Press; 1941.


Investigative Ophthalmology & Visual Science